DINAME 2023 - Proceedings of the XIX International Symposium on Dynamic Problems of Mechanics,
A.S. De Paula, A.T. Fabro and M.R. Machado (Editors), ABCM.
Pirenópolis, Go, Brazil, February 26th to March 3rd, 2023

Gain-Scheduled $\mathscr{H}_2$ Controller for Trajectory Tracking of a Cart-Pendulum

Enzo G. Raffa[1] **and J. F. Camino**[1]

[1]School of Mechanical Engineering, University of Campinas (UNICAMP), Campinas, SP 13083–860, Brazil.
e-mail: enzograffa@gmail.com, camino@fem.unicamp.br

Abstract: This paper presents the design of a gain scheduling controller based on the $\mathscr{H}_2$ performance for trajectory tracking of a cart-pendulum system. The nonlinear dynamics of the cart-pendulum system are used to model an overhead crane. The gain scheduling is a flexible technique that allows a controller to be designed for a nonlinear system based on a set of linearized subproblems. For each operating condition, a local linear controller is designed using the $\mathscr{H}_2$ control problem, in which weighting functions are properly chosen to minimize tracking error and control effort. The resulting local linear controllers are activated according to a scheduling variable. Numerical results show the benefits of the proposed approach.

***Keywords:* gain scheduling, H_2 control, trajectory tracking, cart-pendulum system, overhead crane.**

INTRODUCTION

The cart-pendulum system dynamics can be used as a simplified model for the dynamics of more complex nonlinear mechanical systems, such as the two-dimensional motion of a rocket, the translation of a Segway, among other applications (Hauser et al., 2005). The cart-pendulum system is also commonly used as a simplified model of overhead cranes (Auernig and Troger, 1987; Singhose et al., 2000), which consists of a moving trolley with a payload attached to it by a rope (Fang et al., 2012). As the trolley moves, it creates a pendulum-like swinging motion on the payload, which can be undesired due to the possibility of cargo damage. For higher performance, a fast and precise payload motion is desired (Auernig and Troger, 1987; Fang et al., 2012).

The trajectory tracking problem involves designing a control law that forces the mechanical system to follow a prescribed reference trajectory. This class of control problem is used in everyday applications, such as autonomous quadcopters (Hoffmann et al., 2008; Zuo, 2010; Bonna and Camino, 2015), underwater vehicles (Repoulias and Papadopoulos, 2007), inverted pendulums (Ha et al., 1996), helicopters (Mahony and Hamel, 2004), among others. For overhead cranes, the tracking problem can be used to force the cart or the payload to follow a desired position or velocity profile.

Gain scheduling is a technique used to design controllers for nonlinear systems, that consists in dividing the nonlinear problem into a set of linear subproblems by making successive linearizations at distinct operating conditions and then designing local linear controllers for these operating points (Leith and Leithead, 2000; Rugh and Shamma, 2000). The gain scheduling technique has applications ranging from process control to aerospace engineering. According to Rugh (1991), some advantages of gain scheduling include the possibility of using classical and versatile robust control design techniques to deal with uncertainties and to provide fast response capacity upon changes in operating conditions.

In the gain scheduling approach, any control design strategy can be used to design the local controllers. For our application, the $\mathscr{H}_2$ control problem, that minimizes the $\mathscr{H}_2$ norm of the closed-loop system, is used for the local designs (Doyle et al., 1989; Stoorvogel, 1993; Saberi et al., 1996). The $\mathscr{H}_2$ problem has been largely used in many engineering applications (Rotea, 1993; Wang and Wilson, 2001; Kwakernaak, 2002; De Caigny et al., 2010; Camino and Santos, 2018). To obtain the desired performance and robustness, it is necessary to incorporate appropriately into the design weighting functions to shape the loop gain, the sensitivity, and the complementary sensitivity functions (Grimble and Biss, 1988; Postlethwaite et al., 1990; Zhou and Doyle, 1998).

EQUATION OF MOTION

The dynamics of an overhead crane can be modeled by a cart-pendulum system (Auernig and Troger, 1987; De Caigny et al., 2014), as shown in Figure 1. The cart represents the trolley. The pendulum is composed of a cable with a payload attached to its tip. The mass of the trolley is denoted by M [kg] and its displacement by $q(t)$ [m]. The payload has mass m [kg], and the cable has length l [m]. The angular displacement of the payload is denoted by $\theta(t)$ [rad]. The gravity of the Earth is denoted by g [m/s^2]. An external control force $f(t)$ [N] is applied to the trolley.

The nonlinear equation of motion of the cart-pendulum is given by

$$\begin{aligned}(M+m)\ddot{q}+ml(\ddot{\theta}\cos\theta-\dot{\theta}^2\sin\theta)&=f\\ l\ddot{\theta}+\cos\theta\ddot{q}+g\sin\theta&=0\end{aligned} \tag{1}$$

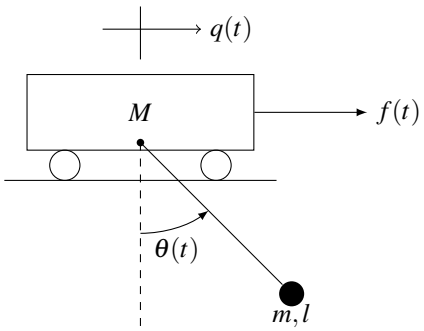

Figure 1 – Cart-pendulum system.

After some manipulations, the equation of motion (1) can be conveniently rewritten as

$$\begin{aligned} a_1\ddot{q} - a_2 - a_3 &= f \\ l a_1 \ddot{\theta} + a_2\cos(\theta) + a_4 &= -f\cos(\theta) \end{aligned}$$

with

$$\begin{aligned} a_1 &= M + m - m\cos^2(\theta) \\ a_2 &= ml\dot{\theta}^2\sin(\theta) \\ a_3 &= mg\sin(\theta)\cos(\theta) \\ a_4 &= (M+m)g\sin(\theta) \end{aligned}$$

Now, by choosing the control force $f(t)$ as

$$f(t) = a_1 u(t) - a_2 - a_3 \tag{2}$$

where $u(t)$ is a new virtual control input, the equation of motion becomes

$$\begin{aligned} \ddot{q}(t) &= u(t) \\ \sec(\theta(t))\ddot{\theta}(t) &= \beta(g\tan(\theta(t)) + u(t)), \qquad \beta = -1/l \end{aligned} \tag{3}$$

This provides a partial feedback linearization of this underactuated system. Note that the translational dynamics in (3) are now linear and decoupled from the rotational dynamics, which still contain nonlinear terms.

PROBLEM FORMULATION

In most conventional applications, it is desired to move the payload at the edge of the cable, whose absolute horizontal displacement $y_p(t)$ is

$$y_p(t) = q(t) + l\sin(\theta(t)), \tag{4}$$

from a rest (initial) position y_0 to a final position y_f in a short time. It is also desired that the payload has a small oscillation during its trajectory to the final position. A convenient way to address this problem is to cast it as a trajectory tracking problem where the payload's absolute horizontal displacement $y_p(t)$ must follow a step reference input with a small overshoot and settling time.

Trajectory tracking problem

Since the goal is to design a controller for the cart-pendulum system that can guarantee trajectory tracking of a step reference input with a small error, the trajectory tracking problem amounts to finding a controller such that

$$\lim_{t\to\infty} |e(t)| < \varepsilon, \qquad \text{for a small } \varepsilon,$$

where the trajectory tracking error $e(t)$ is defined by

$$e(t) = r(t) - y_p(t)$$

where $r(t)$ is the reference trajectory, which hereafter is assumed to be a step of amplitude r.

CONTROL DESIGN

This section presents the proposed trajectory tracking control design using a gain scheduling approach based on the $\mathscr{H}_2$ problem. First, we introduce the gain scheduling technique and the underlying linearization method. Then, we present the derivation of the local models. After that, we present the control system's block diagram for the servomechanism, together with its equivalent generalized plant representation. Finally, we introduce the $\mathscr{H}_2$ control problem that provides the local controllers.

Gain scheduling technique

The gain scheduling technique allows the design of a controller for a nonlinear system by decomposing the problem into several linear subproblems. For the gain-scheduled controller design (Rugh and Shamma, 2000), it is necessary to follow the following steps:

1. Linearize the nonlinear system around a set of operating conditions;
2. For this set of operating conditions, design a local LTI controller for each one of the local linear models;
3. Implement the gain-scheduled controller by alternating among the designed LTI controllers according to a scheduling rule;
4. Finally, check closed-loop system stability and performance.

The equation of motion is linearized using the first-order Taylor series approximation around the operating point $\bar{p}$, as shown below:

$$f(p) \approx f(\bar{p}) + \sum_{i=1}^{n} \left.\frac{\partial f(p)}{\partial p_i}\right|_{p=\bar{p}} (p_i - \bar{p}_i)$$

where $p_i \in \mathbb{R}$ is the i-*th* term of the vector $p \in \mathbb{R}^n$, which contains all the variables of the nonlinear function $f(p) : \mathbb{R}^n \to \mathbb{R}$. Notice that the equation of motion (1) of the cart-pendulum system has several nonlinear terms, which demand more linearizations and, therefore, more operating points than (3), for which the translational dynamics are already linear, and the rotational dynamics contains fewer nonlinear terms, leading to a lower number of operating points.

Local linearized models

Linearizing (3) around the operating point $p = (\bar{\theta}, \ddot{\bar{\theta}})$ leads to

$$\begin{aligned} \ddot{q}(t) &= u(t) \\ \ddot{\theta}(t) &= c_1\theta(t) + c_2 + c_3 u(t) \end{aligned} \tag{5}$$

with the following constant coefficients:

$$\begin{aligned} c_1 &= -\ddot{\bar{\theta}}\tan(\bar{\theta}) + \beta g \sec(\bar{\theta}) \\ c_2 &= \ddot{\bar{\theta}}\tan(\bar{\theta})\bar{\theta} + \beta g \sin(\bar{\theta}) - \beta g \bar{\theta}\sec(\bar{\theta}) \\ c_3 &= \beta\cos(\bar{\theta}) \end{aligned}$$

Now, using the following change of variable:

$$s = \begin{bmatrix} q(t) & \dot{q}(t) & \theta(t) + c_2/c_1 & \dot{\theta}(t) \end{bmatrix}^T$$

system (5) can be written conveniently as

$$\dot{s}(t) = A_p s(t) + B_p u(t)$$

where matrices A_p and B_p are given by

$$A_p = \begin{bmatrix} 0 & 1 & 0 & 0 \\ 0 & 0 & 0 & 0 \\ 0 & 0 & 0 & 1 \\ 0 & 0 & c_1 & 0 \end{bmatrix}, \qquad B_p = \begin{bmatrix} 0 \\ 1 \\ 0 \\ c_3 \end{bmatrix},$$

The linearized payload absolute horizontal displacement around the origin is given by

$$y_p(t) = q(t) + l\theta(t) = s_1 + l(s_3 - c_2/c_1) = C_p s(t) + \bar{y}_p$$

with

$$C_p = \begin{bmatrix} 1 & 0 & l & 0 \end{bmatrix}, \qquad \bar{y}_p = -lc_2/c_1$$

Defining the output of plant G as

$$y_g(t) = y_p(t) - \bar{y}_p = C_p s(t)$$

we obtain the following state-space representation for the local model:

$$G = \begin{bmatrix} A_p & B_p \\ C_p & 0 \end{bmatrix} \tag{6}$$

Notice that the trajectory tracking error now becomes

$$e(t) = r(t) - y_p(t) = r(t) - \bar{y}_p - y_g(t) = \hat{r}(t) - y_g(t), \qquad \hat{r}(t) = r(t) - \bar{y}_p$$

Thus, once $r(t)$, c_1, and c_2 are known, $\bar{y}_p$ is known, and hence $\hat{r}(t)$ is also known. So, a controller designed for the local model (6) such that $y_g(t)$ tracks $\hat{r}(t)$, enforces that $y(t)$ tracks $r(t)$ and, therefore, $e(t)$ is minimized.

Control system's block diagram and generalized plant

Figure 2 shows the control system's block diagram for the proposed trajectory tracking problem. The weighting functions on the tracking error and the control effort are denoted by W_e and W_u, respectively. These weights penalize e and u in certain frequency range and shape the sensitivity function. In this figure, K is the local controller, G is the local linearized model of the cart-pendulum system, given by (6), $\tilde{e}$ is the weighted trajectory tracking error, and $\tilde{u}$ is the weighted control effort. It is worth emphasizing that the same weighting functions W_e and W_u are used for all the local models. Eventually, in a more elaborate design, the weighting functions can be chosen differently for each local model.

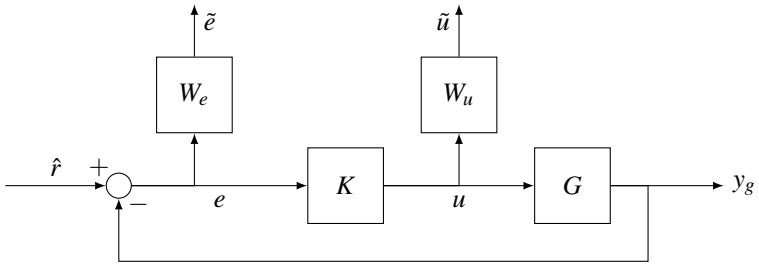

Figure 2 – Control system's block diagram.

The trajectory tracking problem presented in Figure 2 will now be solved using the $\mathscr{H}_2$ control problem. For this purpose, it is necessary to represent the control system's block diagram from Figure 2 in the well know generalized plant configuration shown in Figure 3.

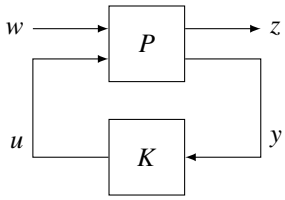

Figure 3 – Generalized plant.

Observing from Figure 2 that

$$y_g = Gu, \qquad u = Ke, \qquad e = \hat{r} - y_g, \qquad \tilde{u} = W_u u, \qquad \tilde{e} = W_e e$$

and defining the signals of the generalized plant as

$$z = \begin{bmatrix} \tilde{e} \\ \tilde{u} \end{bmatrix} = \begin{bmatrix} W_e e \\ W_u u \end{bmatrix}$$
$$y = e = \hat{r} - y_g$$
$$w = \hat{r}$$

the following equations are obtained:

$$z = \begin{bmatrix} W_e w - W_e G u \\ W_u u \end{bmatrix}$$
$$y = w - Gu$$

Now, noticing that the generalized plant $P(s)$ relates the output vector $[z^T \ y^T]^T$ with the input vector $[w^T \ u^T]^T$, one finally obtains

$$P(s) = \begin{bmatrix} W_e & -W_e G \\ 0 & W_u \\ I & -G \end{bmatrix} \tag{7}$$

Clearly, $P(s)$ can also have a state-space representation in the form:

$$\begin{aligned} \dot{x}(t) &= Ax(t) + B_1 w(t) + B_2 u(t) \\ z(t) &= C_1 x(t) + D_{11} w(t) + D_{12} u(t) \\ y(t) &= C_2 x(t) + D_{21} w(t) + D_{22} u(t) \end{aligned} \tag{8}$$

where $x(t)$ is the state vector of the generalized plant, composed of the state vector $s(t)$ of the plant G, the state vector $x_e(t)$ of the weight function W_e and the state vector $x_u(t)$ of the weight function W_u. The vector $z(t)$ is the performance output signal, $y(t)$ is the measurement output signal, $w(t)$ is the exogenous input signal, and $u(t)$ is the control input signal. Matrices A, B_1, B_2, C_1, C_2, D_{11}, D_{12}, D_{21}, and D_{22} have compatible dimensions and are given in the Appendix.

The $\mathscr{H}_2$ control problem

The $\mathscr{H}_2$ control problem (see Rotea (1993); Zhou and Doyle (1998)) provides a controller K that minimizes the $\mathscr{H}_2$ norm of the closed-loop transfer function relating the output signal z to the input signal w for the generalized plant from Figure 3, in which, the $\mathscr{H}_2$ norm of a strictly proper transfer function $H(s)$ is defined as

$$||H(s)||_2^2 = \frac{1}{2\pi} \int_{-\infty}^{\infty} \mathrm{Tr}\left\{H(j\omega)^H H(j\omega)\right\} d\omega$$

where $H(j\omega)^H$ denotes the complex conjugate transpose of $H(j\omega)$.

In the hypotheses for the existence of the optimal $\mathscr{H}_2$ controller, it is assumed that D_{11} is zero to guarantee that the $\mathscr{H}_2$ problem is properly posed and that D_{22} is zero so that the transfer function $\mathrm{P}_{22}(s)$ is strictly proper. It is also necessary to assume that:

- the pair (A, B_2) is stabilizable, and the pair (A, C_2) is detectable;
- matrices $R_1 = D_{12}^T D_{12} > 0$ and $R_2 = D_{21} D_{21}^T > 0$;
- matrix $\begin{bmatrix} A - j\omega I & B_2 \\ C_1 & D_{12} \end{bmatrix}$ has full column rank for all ω and matrix $\begin{bmatrix} A - j\omega I & B_1 \\ C_2 & D_{21} \end{bmatrix}$ has full row rank for all ω.

Under these hypotheses, the solution of the optimal $\mathscr{H}_2$ control problem is obtained by solving the following two algebraic Riccati equations:

$$(A - B_2 R_1^{-1} D_{12}^T C_1)^T X + X(A - B_2 R_1^{-1} D_{12}^T C_1) - X B_2 R_1^{-1} B_2^T X + C_1^T (I - D_{12} R_1^{-1} D_{12}^T) C_1 = 0$$
$$(A - B_1 D_{21}^T R_2^{-1} C_2) Y + Y (A - B_1 D_{21}^T R_2^{-1} C_2)^T - Y C_2^T R_2^{-1} C_2 Y + B_1 (I - D_{21}^T R_2^{-1} D_{21}) B_1^T = 0$$

with

$$X = X^T \geq 0, \qquad Y = Y^T \geq 0$$

Once X and Y are computed, the two gains F_2 and L_2 are given by

$$F_2 = -R_1^{-1}(B_2^T X + D_{12}^T C_1) \quad \text{and} \quad L_2 = -(Y C_2^T + B_1 D_{21}^T) R_2^{-1}$$

and the optimal $\mathscr{H}_2$ controller is given by the following state-space representation

$$K = \begin{bmatrix} A + B_2 F_2 + L_2 C_2 & -L_2 \\ F_2 & 0 \end{bmatrix}$$

NUMERICAL RESULTS

This section first presents an analysis of two local closed-loop systems computed at two distinct operating conditions and, afterward, the numerical results for the nonlinear cart-pendulum system in closed-loop using the gain-scheduled controller. For all designs and simulations in this section, the overhead crane numerical parameters, taken from Fang et al. (2012), are given by

$$M = 6.5\,[\text{kg}], \qquad m = 1.025\,[\text{kg}], \qquad l = 0.6\,[\text{m}], \qquad g = 9.81\,[\text{m/s}^2]$$

All initial conditions are assumed to be zero, and the weighting functions W_e and W_u are given by

$$W_e(s) = 10^4 \frac{(s+49.45)(s+4.55)}{(s+10^4)(s+54)(s+10^{-6})}, \qquad W_u(s) = 6\frac{s+10}{s+10^3}$$

The operating points used for the gain scheduling design are

$$\bar{\theta} = [-20,\ -10,\ 0,\ 10,\ 20] \qquad \text{and} \qquad \ddot{\bar{\theta}} = [-400,\ -200,\ 0,\ 200,\ 400]$$

Notice that, these points provide a total of 25 local linearized models and consequently 25 local LTI $\mathscr{H}_2$ controllers.

Closed-loop with the local linearized models

This section presents numerical simulations of two local closed-loop systems computed at two distinct operating conditions. For the first set of numerical simulations, a local LTI controller is designed using the $\mathscr{H}_2$ control problem for the nonlinear model (3) linearized at the origin, i.e., at the operating point $\bar{\theta} = 0$ and $\ddot{\bar{\theta}} = 0$. The next two figures show the results of the respective local closed-loop system to a unit step reference input. Figure 4 shows the payload absolute horizontal displacement $y_p(t)$ [m], the trolley displacement $q(t)$ [m], and the payload angular displacement $\theta(t)$ [degree]. Figure 5 presents the tracking error $e(t)$ [m] and the force $f(t)$ [N] applied to the trolley.

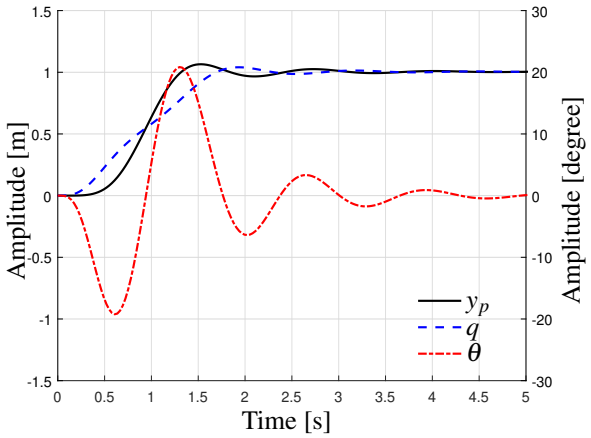

Figure 4 – $y_p(t)$, $q(t)$, $\theta(t)$ **for** $(\bar{\theta}, \ddot{\bar{\theta}}) = (0,0)$.

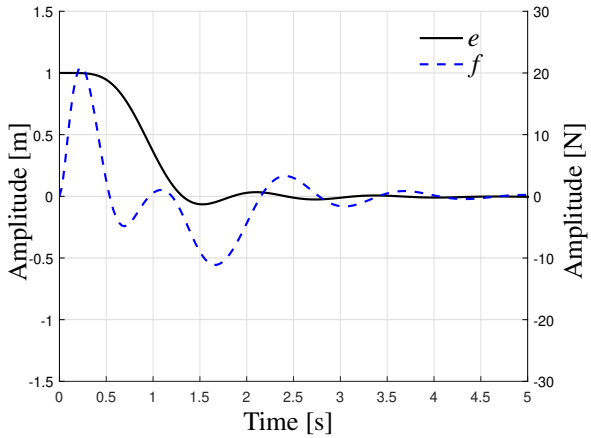

Figure 5 – $e(t)$, $f(t)$ **for** $(\bar{\theta}, \ddot{\bar{\theta}}) = (0,0)$.

Observe that the payload absolute horizontal displacement $y_p(t)$ can track a unit step reference input with a settling time of 2.88 [s] and an overshoot of 6.54%, approximately. To achieve that fast response, i.e., small settling time with small overshoot, the payload initially undergoes a large swing, around 21 [degree] in absolute value. This is an inherent trade-off imposed by this type of underactuated mechanical system. Notice also that the maximum force $f(t)$ applied to the trolley was close to 21 [N] and the maximum trolley displacement $q(t)$ was close to 1.04 [m].

For the second local design, the operating condition is chosen as $\bar{\theta} = -10$ and $\ddot{\bar{\theta}} = 200$. The results of the respective local closed-loop system to a unit step reference input are shown in the next two figures. Figure 6 shows the payload absolute horizontal displacement $y_p(t)$ [m], the trolley displacement $q(t)$ [m], and the payload angular displacement $\theta(t)$ [degree]. Figure 7 presents the tracking error $e(t)$ [m] and the force $f(t)$ [N] applied to the trolley.

Again, the local closed-loop system is able to track a unit step reference input with a fast settling time of 2.91 [s] and a small overshoot of about 6.76%. The maximum angular displacement of the payload was 20.98 [degree] in absolute value, the maximum trolley displacement was again 1.04 [m], and the maximum force applied to the trolley was about 21 [N]. Compared to the performance of the previous local model, linearized at the origin, both settling time and overshoot increased. However, the extent to which they increased was insignificant. Similar results were obtained for all the other operating conditions used in the design of the local controllers for the gain-scheduled controller. Thus, all local $\mathscr{H}_2$ controllers provided satisfactory closed-loop performance.

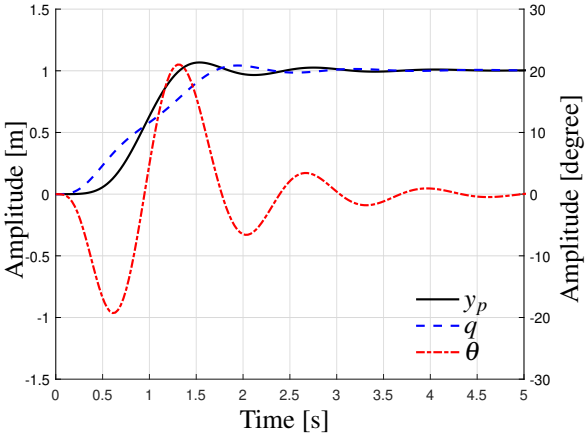

Figure 6 – $y_p(t), q(t), \theta(t)$ **for** $(\bar{\theta}, \ddot{\bar{\theta}}) = (-10, 200)$**.**

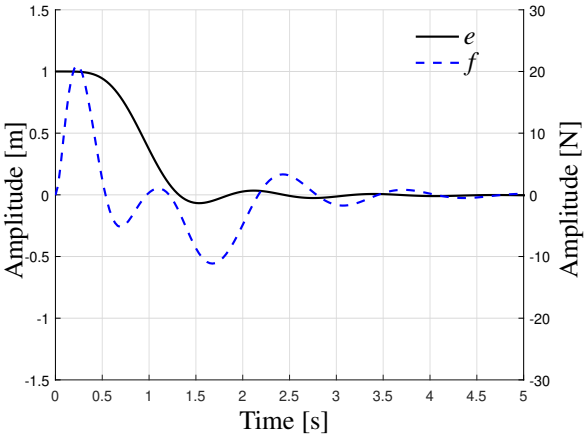

Figure 7 – $e(t), f(t)$ **for** $(\bar{\theta}, \ddot{\bar{\theta}}) = (-10, 200)$**.**

Closed-loop with the nonlinear cart-pendulum system

This section presents the numerical results of the cart-pendulum system in closed-loop with the proposed gain-scheduled controller. Figure 8 shows the control system's block diagram, representing the nonlinear cart-pendulum system, given by (1), with its actuation law, given by (2), in closed-loop with the gain-scheduled controller denoted by GS.

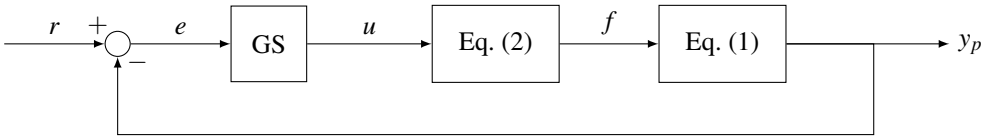

Figure 8 – Control system's block diagram with nonlinear plant and gain-scheduled controller.

Although in many practical implementations, a gain-scheduled controller is formed by interpolating between the set of linear controllers derived for the corresponding set of linearized models associated with several operating points, in this paper, our gain-scheduled controller GS works by activating a specific local controller once both scheduling variables $\theta(t)$ and $\ddot{\theta}(t)$ reach the operating region for which the respective local controller was designed to work.

The next two figures show the system's closed-loop response to a unit step reference input with zero initial condition. Figure 9 shows the payload absolute horizontal displacement $y_p(t)$ [m], the trolley displacement $q(t)$ [m], and the payload angular displacement $\theta(t)$ [degree]. Figure 10 presents the tracking error $e(t)$ [m] and the force applied to the trolley $f(t)$ [N]. It is possible to observe that the tracking error approaches zero, the overshoot of the overhead crane payload displacement is negligible, and the settling time is small, implying that the proposed gain-scheduled controller achieved the desired performance.

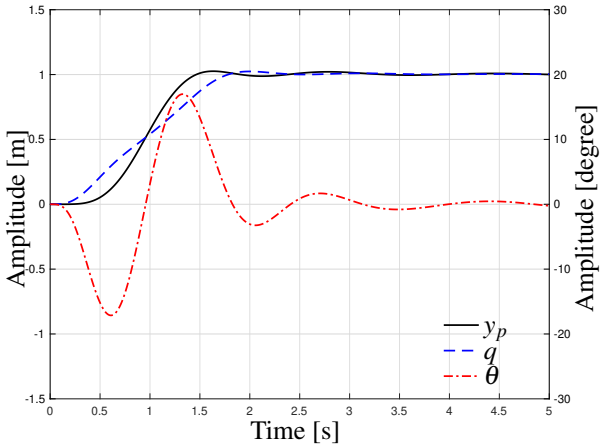

Figure 9 – $y_p(t), q(t), \theta(t)$ **for nonlinear plant.**

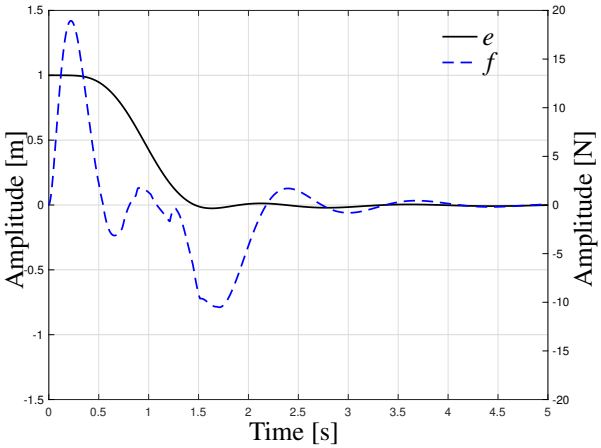

Figure 10 – $e(t), f(t)$ **for nonlinear plant.**

CONCLUSIONS

This paper shows that it is possible to make the overhead crane payload displacement follow a step reference with a small settling time and overshoot using the gain scheduling control technique. The $\mathscr{H}_2$ control problem was used to design the local controllers. All local linearized models achieved stringent closed-loop performance. The proposed gain-scheduled controller that works by activating the local $\mathscr{H}_2$ controllers also provided satisfactory performance. Although robustness to uncertainty was not addressed in this paper, this issue can be conveniently incorporated into the $\mathscr{H}_2$ formulation. Another important aspect that can be further investigated is the application of the proposed gain scheduling technique to cope with the variation of the cable's length that carries the load.

REFERENCES

Auernig, J. W. and Troger, H. (1987). Time optimal-control of overhead cranes with hoisting of the load. *Automatica*, 23(4):437–447.

Bonna, R. and Camino, J. F. (2015). Trajectory tracking control of a quadrotor using feedback linearization. In *Proceedings of the 17th International Conference on Dynamic Problems in Mechanics*, pages 1–09, Natal, RN, Brazil.

Camino, J. F. and Santos, I. F. (2018). A periodic $\mathscr{H}_2$ state feedback controller for a rotor-blade system. In *Proceedings of the International Conference on Noise and Vibration Engineering*, pages 3413–3425, Leuven, Belgium.

De Caigny, J., Camino, J. F., Oliveira, R. C. L. F., Peres, P. L. D., and Swevers, J. (2010). Gain-scheduled $\mathscr{H}_2$ and $\mathscr{H}_\infty$ control of discrete-time polytopic time-varying systems. *IET Control Theory & Applications*, 4(3):362–380.

De Caigny, J., Pintelon, R., Camino, J. F., and Swevers, J. (2014). Interpolated modeling of LPV systems. *IEEE Transactions on Control Systems Technology*, 22(6):2232–2246.

Doyle, J. C., Glover, K., Khargonekar, P. P., and Francis, B. A. (1989). State-space solution to standard H_2 and H_∞ control problems. *IEEE Transactions on Automatic Control*, 34(8):831–847.

Fang, Y., Ma, B., Wang, P., and Zhang, X. (2012). A motion planning-based adaptive control method for an underactuated crane system. *IEEE Transactions on Control Systems Technology*, 20(1):241–248.

Grimble, M. J. and Biss, D. (1988). Selection of optimal control weighting functions to achieve good H_∞ robust designs. In *1988 International Conference on Control*, pages 683–688, Oxford, UK.

Ha, Y.-S. et al. (1996). Trajectory tracking control for navigation of the inverse pendulum type self-contained mobile robot. *Robotics and autonomous systems*, 17(1-2):65–80.

Hauser, J., Saccon, A., and Frezza, R. (2005). On the driven inverted pendulum. In *Proceedings of the 44th IEEE Conference on Decision and Control*, pages 6176–6180.

Hoffmann, G., Waslander, S., and Tomlin, C. (2008). Quadrotor helicopter trajectory tracking control. In *AIAA guidance, navigation and control conference and exhibit*, pages 18–21.

Kwakernaak, H. (2002). $H2$-optimization — Theory and applications to robust control design. *Annual Reviews in Control*, 26(1):45–56.

Leith, D. J. and Leithead, W. E. (2000). Survey of gain-scheduling analysis and design. *International Journal of Control*, 73(11):1001–1025.

Mahony, R. and Hamel, T. (2004). Robust trajectory tracking for a scale model autonomous helicopter. *International Journal of Robust and Nonlinear Control*, 14(12):1035–1059.

Postlethwaite, I., Tsai, M.-C., and Gu, D.-W. (1990). Weighting function selection in H_∞ design. In *11th IFAC World Congress on Automatic Control*, pages 127–132, Tallinn, Finland.

Repoulias, F. and Papadopoulos, E. (2007). Planar trajectory planning and tracking control design for underactuated AUVs. *Ocean engineering*, 34(11-12):1650–1667.

Rotea, M. (1993). The generalized H_2 control problem. *Automatica*, 29(2):373–385.

Rugh, W. J. (1991). Analytical framework for gain scheduling. *IEEE Control Systems Magazine*, 11(1):79–84.

Rugh, W. J. and Shamma, J. S. (2000). Research on gain scheduling. *Automatica*, 36(10):1401–1425.

Saberi, A., Sannuti, P., and Stoorvogel, A. A. (1996). $H2$ optimal controllers with measurement feedback for continuous-time systems — Flexibility in closed-loop pole placement. *Automatica*, 32(8):1201–1209.

Singhose, W., Porter, L., Kenison, M., and Kriikku, E. (2000). Effects of hoisting on the input shaping control of gantry cranes. *Control Engineering Practice*, 8(10):1159–1165.

Stoorvogel, A. A. (1993). The robust $\mathscr{H}_2$ control problem: A worst-case design. *IEEE Transactions on Automatic Control*, 38(9):1358–1370.

Wang, J. and Wilson, D. A. (2001). Mixed $GL_2/H_2/GH_2$ control with pole placement and its application to vehicle suspension systems. *International Journal of Control*, 74(13):1353–1369.

Zhou, K. and Doyle, J. C. (1998). *Essentials of Robust Control*. Prentice-Hall, Upper Saddle River, USA.

Zuo, Z. (2010). Trajectory tracking control design with command-filtered compensation for a quadrotor. *IET control theory & applications*, 4(11):2343–2355.

RESPONSIBILITY NOTICE

The author(s) is (are) the only responsible for the printed material included in this paper.

APPENDIX

State-space representation of the generalized plant P

To derive the state-space representation of the generalized plant P, that represents the control system's block diagram from Figure 2, the transfer functions W_e, W_u, and G are assumed to have the following state-space representation: the weighting function W_e is given by

$$\begin{aligned}\dot{x}_e(t) &= A_e x_e(t) + B_e e(t)\\ \tilde{e}(t) &= C_e x_e(t) + D_e e(t)\end{aligned}$$

the weighting function W_u is given by

$$\begin{aligned}\dot{x}_u(t) &= A_u x_u(t) + B_u u(t)\\ \tilde{u}(t) &= C_u x_u(t) + D_u u(t)\end{aligned}$$

and plant G is given by

$$\begin{aligned}\dot{s}(t) &= A_p x_u(t) + B_p u(t)\\ y_g(t) &= C_p s(t) + D_p u(t)\end{aligned}$$

Using these models, the state-space representation of the generalized plant P can be shown to be

$$\begin{bmatrix}\dot{x}\\ z\\ y\end{bmatrix} = P\begin{bmatrix}x\\ w\\ u\end{bmatrix}, \qquad P = \begin{bmatrix}A & B_1 & B_2\\ C_1 & D_{11} & D_{12}\\ C_2 & D_{21} & D_{22}\end{bmatrix}$$

with the system matrices given by

$$A = \begin{bmatrix}A_p & 0 & 0\\ -B_e C_p & A_e & 0\\ 0 & 0 & A_u\end{bmatrix}, \qquad B_1 = \begin{bmatrix}0\\ B_e\\ 0\end{bmatrix}, \qquad B_2 = \begin{bmatrix}B_p\\ -B_e D_p\\ B_u\end{bmatrix}, \qquad C_1 = \begin{bmatrix}-D_e C_p & C_e & 0\\ 0 & 0 & C_u\end{bmatrix}$$

$$C_2 = \begin{bmatrix}-C_p & 0 & 0\end{bmatrix}, \qquad D_{11} = \begin{bmatrix}D_e\\ 0\end{bmatrix}, \qquad D_{12} = \begin{bmatrix}-D_e D_p\\ D_u\end{bmatrix}, \qquad D_{21} = I, \qquad D_{22} = -D_p$$